16th ICAAR LISBOA 2020-2022
16th International Conference on Alkali-Aggregate Reaction in Concrete
Lisboa | LNEC | Portugal | 31 May - 2 June 2022
http://icaar2020-2022.lnec.pt

Report on Load resistant capacity when promoting curing PC Beam specimens affected by Alkali silica reaction

Munenobu Murasaka [(1)], Motoyuki Suzuki [(2)], Sunao Yoshida[(3)]
(1) SUIKUSHA Co., Ltd. , Tokyo, Japan, sks-murasaka@joesei.com
(2) Professor Emeritus Tohoku University, Miyagi, Japan, motoyuki.suzuki.a2@tohoku.ac.jp
(3) Sata Consultants Co., Ltd. , Fukuoka, Japan, sks-murasaka@joesei.com

Abstract
The authors obtained the following opinion in order to evaluate the change in the load-bearing performance of the PC girder during the ASR deterioration process. First, a PC beam specimen was prepared using ASR aggregate,①By carrying out the accelerated curing test, how the PC beam specimen expands, strain and displacement were monitored, and the deterioration grade by ASR was classified.②A loading test was performed for each deterioration grade to evaluate the load-bearing performance of the PC beam specimen. ③Using Broadband ultrasonic, we clarified the frequency characteristics of propagation inside concrete and evaluated the effect of the ASR expansion behavior on the PC beam specimen.In order to confirm the validity of this content, the reproducibility was verified using a railway PC track girder whose ASR progress was confirmed.As a result, the following contents were confirmed and the management method was able to be established. ④From the monitoring results of the strain and the displacement, a similar tendency of the ASR expansion behavior obtained in the test specimen was confirmed. ⑤From the frequency characteristics of the Broadband ultrasonic propagated inside the concrete, it was confirmed that the prestress effect by the PC had the effect of delaying the ASR expansion. This also matched the tendency obtained with the PC beam specimen. ⑥From the displacement waveform obtained in the newly performed dynamic loading test of the fixed load, it was possible to grasp the change in the impact effect due to the progress of ASR. From the displacement waveform obtained in the newly performed dynamic loading test of the fixed load, it was possible to grasp the change in the impact effect due to the progress of ASR. This periodicity means the natural vibration period of the structure itself, and the ASR deterioration process could be evaluated by monitoring this period change.

Keywords:*PC girder, Load-bearing performance, Broadband ultrasonic, Frequency characteristics, Natural period*

1. Introduction (Research Background)
The Kitakyushu Monorail opened in 1985 as a straddle-type monorail line connecting the Kokura-Kita Ward, which is the center of the government-designated city of Kitakyushu, and Kokura-Minami Ward, which has an increasing population, with a total length of 8.8 km.The standard elevated type consists of RC columns and PC track girders [standard span 20.0m, width 85.0cm, height 150cm], and steel columns and steel track girders are used in special sections such as intersections and railway intersections.

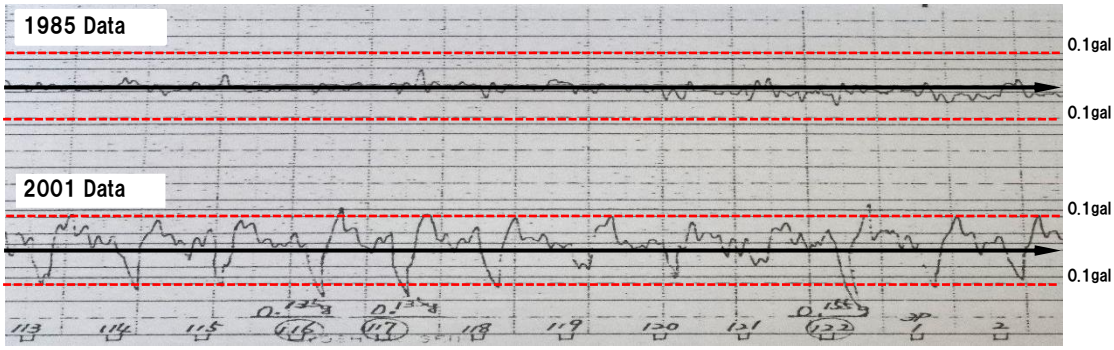

Figure 1: Train acceleration waveforms performed periodically(Vertical direction)

Around 1991, some PC track girders were found to have crack damage, and as can be seen from the periodic train acceleration vibration measurements (Figure 1), the tendency of the acceleration value in the vertical direction to increase became remarkable. A detailed investigation in 2002 revealed that the main cause of the deterioration was the alkali silica reaction (hereinafter referred to ASR).

Generally, PC structures are often used to increase the durability of concrete. It has been considered that the concrete that has generated ASR cracks, thereby significantly decreasing its durability. However, the relationship between the load capacity of each deterioration grade due to the progress of ASR has not been clarified.

In this paper, first, a core specimen using ASR aggregate was prepared, and then accelerated curing was performed. Degradation grades were classified by examining the relationship between expansion coefficient, compressive strength and static elastic modulus. Next, a PC beam specimen was prepared using the same concrete combination, and the expansion behavior due to accelerated curing was monitored from the viewpoint of strain. At the same time, a loading [destruction] test was performed on PC beam specimens for each deterioration grade, and the P-δ curve of the specimens was clarified to verify the load-bearing performance. Before conducting the loading test, a Broadband ultrasonic was propagated to grasp the internal state of the specimen, and the crack propagation progress was evaluated by evaluating the frequency characteristics. Based on the results of these test specimens, we established an evaluation method for the load-bearing performance of PC girder accompanying ASR progress, and applied it to the actual Kitakyushu monorail PC track girder.

2. Classification of degradation grades using core specimens

2.1 Concrete combination (characteristics of reactive aggregate)

Table 1: Concrete mix

W/C (%)	Fine aggregate rate (%)	The unit quantity (kg/m^3)						
		Water (W)	Cement (C)	Fine aggregate nonreactive	Coarse aggregate※1		Water Reducing agent ※3	Alkali immutable weight control ※4
					Reactive ※2	Nonreactive		
46.1	46.8	181	393	855	486	487	C*1.50%	6.0

※1 Grain size range of the coarse aggregate diameter；10～20mm

※2 Ballast-Andesite（The density：2.66g/cm^3, The coefficient of water absorption：3.47%, The coarse rate：6.68）

※3 Protracted type naphthalene system high-range water reducing agent

※4 NaOH was used and added so that the total amount of alkali = 6.0kg/m^3

Table 2 shows the concrete combination used. The reactive aggregate determined to be "no harmless" by the chemical method was an andesite-based aggregate produced in Zhejiang Province, China, and used in a 1:1 ratio with the non-reactive aggregate. Regardless of the reactive aggregate used, it was reported that significant expansion was observed when the total amount of alkali in concrete was 4.0kg/m^3 or more[1]. In this paper, the total amount of alkali was set to 6.0kg/m^3.The core specimens of φ100x200mm were sealed and cured at 20℃ for 5 weeks after the concrete was installation, then immersed in saturated sodium chloride aqueous solution and accelerated curing in a 40℃ constant temperature bath according to the Danish method. The expansion coefficient of the core specimen was calculated from the length measurement by the contact gauge method specified in JIS A 1129$_{1993}$. The specimen having reached a predetermined expansion coefficient was conducted to an ultrasonic transmission test and then to a compressive strength test (JIS A 1108$_{1999}$) including a static elastic modulus test (JIS A 1149$_{2001}$).

2.2 Quantification of material degradation during ASR expansion process

Figure 2 shows the results of the residual swelling test of the core specimen by accelerated curing. Data is measured on a weekly basis. As a characteristic, the expansion rate was slowly (This period is the incubation period) from the start of the measurement to the about 28th day, and the expansion rate was rapidly increased (This period is the accelerated period) by the 28th to 91th days. From the 91st day onward, the expansion rate gradually increased (This period is the deterioration period), confirming that the increasing trend had converged.

Figure 3 and 4 show the results of the expansion rate, compressive strength and static elasticity coefficient test. As the expansion rate increased, both the compressive strength and the static elastic modulus tended to decrease. In particular, it was confirmed that the decreasing rate of the static elastic modulus was large. The static elastic modulus tends to increase when the expansion rate is around 0.04% (Incubation period), and it is considered that the expansion pressure resulting from the volume expansion accompanying the ASR reaction was accumulated inside the aggregate. From the above results, it was confirmed that both the compressive strength and the static elastic modulus were maintained at a high level during the incubation period, turned to decrease during the acceleration period, and converged from the latter half of the acceleration period to the deterioration period.

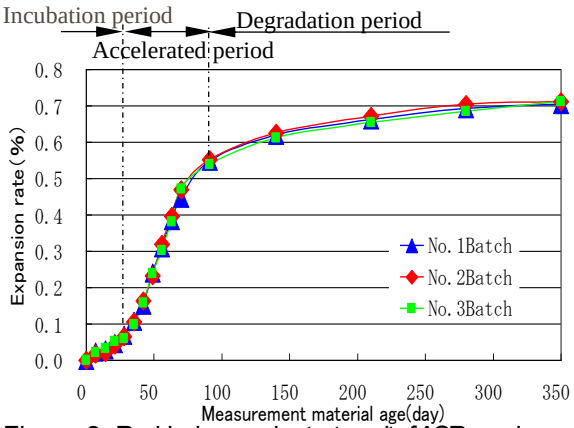

Figure 2: Residual expansion test result of ASR specimen

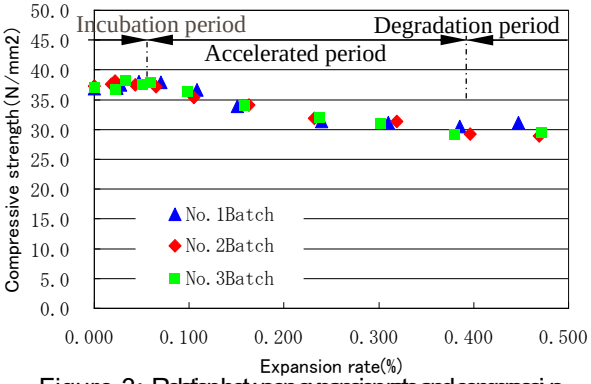

Figure 3: Relation between expansion rate and compressive

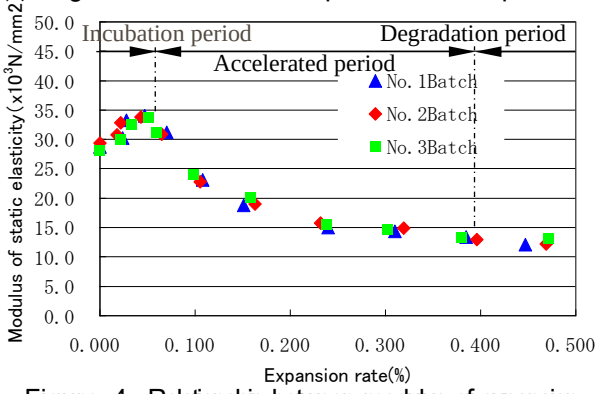

Figure 4: Relationship between modulus of expansion and static elastic modulus

3. Experimental results using PC beam specimen

3.1 Outline of PC beam specimen

The PC beam specimen (hereinafter referred to specimen) was made into a girder form with a rectangular cross section in consideration of performing a loading test. In the specimen, a strain gauge for monitoring, a strain gauge, and a displacement gauge were arranged on the PC steel material and reinforcing steel shown in Figure 5, and a normal design level of tension was applied.The specimen was cured on site for about one month after installation, and after confirming that the concrete had reached the specified strength, prestress was introduced and grouting was performed. The prestress force to be introduced was determined so that the prestress force at the time of the experiment was about 60% of the standard tensile load of the PC steel.Table 2 shows the standard values and prestress target values for the PC steel used.

Table 3 shows the types of test specimens. For the test specimens, a reference sound model [№0] was produced by referring to the deterioration grade obtained from the core test specimen above, and one specimen at a time corresponding to the incubation period (№1), acceleration period (№2), deterioration period①(№3), deterioration period②(№4) was manufactured one by one. Later, a loading test was conducted. After the loading test, cores were sampled from the position shown in Figure 5 (▨) and a compression strength test including a static elastic modulus test was performed. The reason for preparing two specimens during the deterioration period is as follows. As shown in Figure 6 below, the strain caused by accelerated curing turned to a decreasing trend after the maximum strain was confirmed, and a tendency to converge was confirmed. Therefore, it was manufactured to confirm how this difference affected the load carrying performanc.

3.2 Monitoring measurement result by accelerated curing test

Specimens were subjected to accelerated curing (set to a temperature of 40℃ and a humidity of 98% or more) in an environment room to reproduce ASR degradation. The measurement was performed for four items : ①Distance between two points (between A-B/C-D) ②Displacement of the upper and lower surfaces at the center of the span ③Upper and lower edge axial reinforcement strain ④PC steel strain. The start time of the accelerated curing was defined as the initial, and the results for ① to ④ were

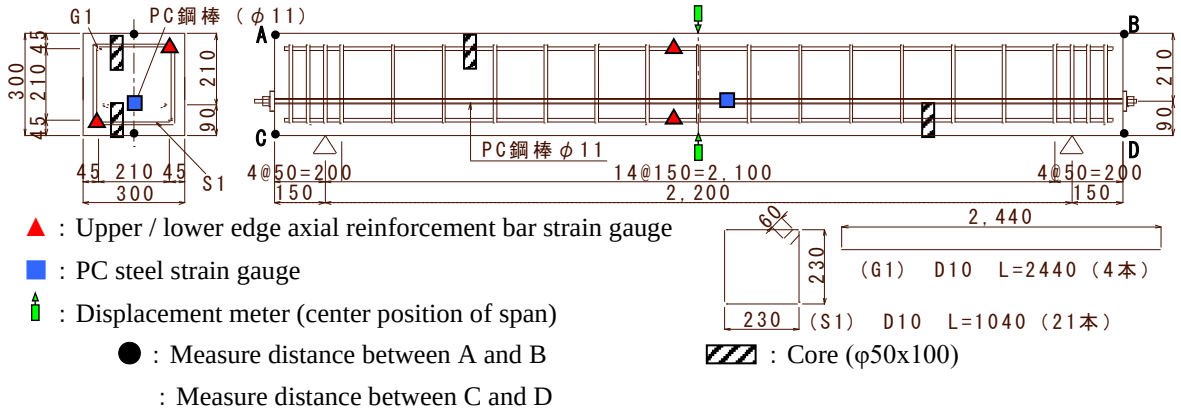

Figure 5: Bar arrangement drawing of PC beam specimen and Strain gauge/Displacement meter installation position diagram

measured every 10 minutes for a total of 700 days. When plotting, the data was specified every two weeks. In ①, the distance between two points was measured with a laser distance meter, and the other data was automatically measured with a data logger.

Table 2: Standard values and prestress target values(SBPR1080/1230)

Diameter bar;mm	Sectional area Ap;mm²	Tensile strength σpu;N/mm²	Target stress level 0.6σpu;N/mm²	Target tension 0.6pu;kN
11	95.03	1230	738	70.13

Table 3: Specimen type

Specimen name	Dimensions (mm)	Degradation process to carry out the load test				
		Sound model	Incubation period	Accelerated period	Degradation period①	Degradation Period②
No.0	300x300 x2500	●				
No.1			●			
No.2				●		
No.3					●	
No.4						●

Figure 6 shows the results of monitoring the distance between the upper and lower edges of the specimen (hereinafter referred to, concrete surface strain) by accelerated curing. After the upper edge strain expanded, when the behavior turned to the convergence tendency, the lower edge strain tended to expand. This tendency was confirmed by the behavior of the span center displacement shown in Figure 7. Also, it can be confirmed that the upper edge strain is larger than the lower edge strain due to the eccentric arrangement of the PC steel material.From this result, in the expansion step of the PC beam specimen by ASR, no noticeable expansion can be confirmed in the incubation period, when the acceleration period begins, the expands significantly in the axial direction of the upper edge (points A and B) where both ends are not restricted, and concurrently expands vertically upward. On the other hand, the lower edge hardly expands due to the prestressing force of the PC steel. When the expansion on the upper edge side stops, the expansion power of the ASR overcomes the prestressing force of the PC steel on the lower edge side and expands

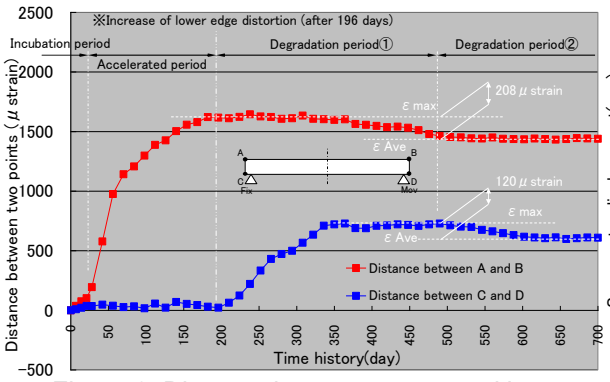

Figure 6: Distance between upper and lower edge surfaces 2 points (strain)

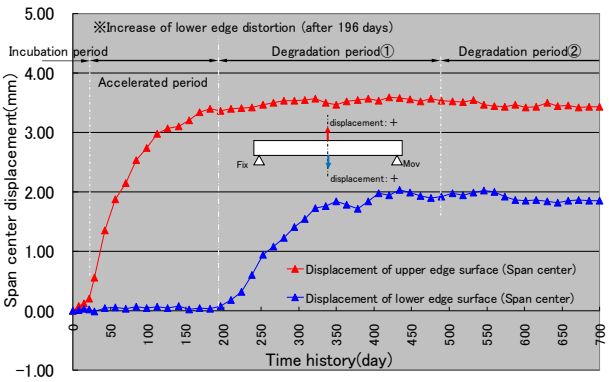

Figure 7: Span center displacement between upper and lower edge faces

in the axial direction. At the same time, it could be judged that it swelled vertically, though not so much upward.

Figure 8 shows the results of monitoring the strain behavior of the upper and lower edge axial reinforcement and PC steel inside the specimen by accelerated curing. Although the upper and lower edge strains in Figure 6 could be confirmed, the elongation of the upper edge axial reinforcement strain tended to slow down after 200 days, while the lower edge axial reinforcement strain and PC steel strain tended to increased. In previous papers[2], there is a report of an increase in upper edge axial reinforcement strain, but no report of an increase in lower edge strain or PC steel strain. Probably, the upper edge side concrete expands due to ASR deterioration by accelerated curing. If the expansion tendency calms down at a certain stage, it is considered that the lower edge side concrete, which had been constrained by the prestressing force of the PC steel material, expanded by overcoming the prestressing f orce. After the maximum strain is confirmed on both the upper and lower edges, a decreasing tendency is observed. The upper edge axial reinforcement strain is decreased by about 25% and the lower edge axial reinforcement strain is decreased by about 35% with respect to the maximum strain. On the other hand, the PC steel strain did not show a large decreasing tendency.

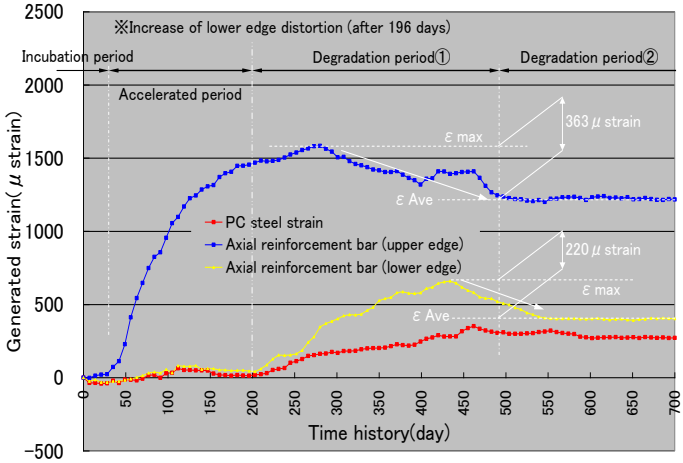

Figure 8: PC steel and upper and lower edge axial reinforcement bar strain

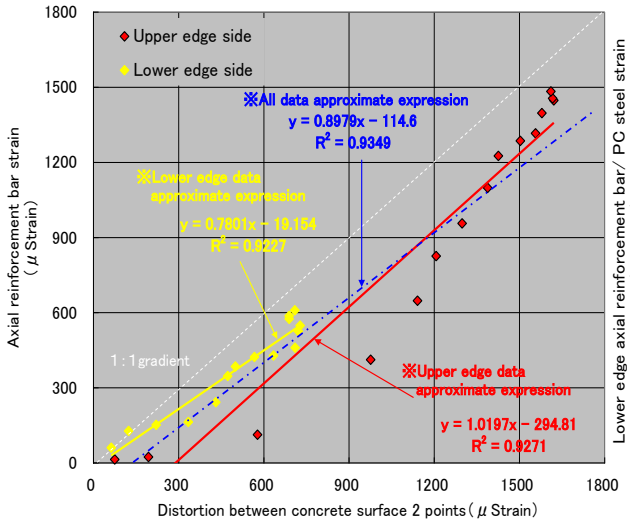

Figure 9: Relationship between Concrete surface strain and Axial reinforcement bar strain

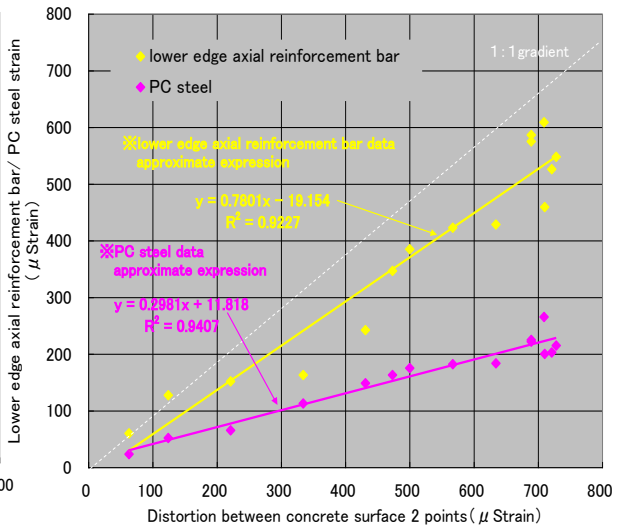

Figure 10: Relationship between Concrete surface strain and Lower edge axial reinforcement bar strain・PC steel strain

Figure 9 shows the relationship between the strain (concrete surface strain) between two points on the upper and lower edges of concrete and the axial reinforcement strain. At both the upper and lower edges, there is a tendency that the axial reinforcement strain is basically proportional to the concrete surface strain, and the slope of the approximate expression based on all data is "0.898", and it can be confirmed that the correlation with " R^2=0.9349" is very high.This indicates that the axial reinforcement strain and the concrete surface strain tend to synchronize. Accordingly, if the concrete surface strain can be grasped, it can be determined that the strain of the internal axial reinforcement can be grasped.

Figure 10 shows the relationship between the surface strain of concrete and the strain of the lower edge axial reinforcement and PC steel. As described above, the lower-edge axial reinforcement strain and the concrete surface strain tend to synchronize, and it can be confirmed that the slope of the approximation formula is close to 1:1 with “0.780”. Although the PC steel strain is proportional to the concrete surface strain, the slope of the approximate formula is “0.299”, and it can be confirmed that the strain increasing tendency is slower than that of the axial reinforcement. This is considered to be the effect of the PC steel material being restrained by the prestressing force introduced.

3.3 Verification of load capacity (destruction) by loading test

In the loading test (destruction), a two-point concentrated load system symmetric to a simple beam with a specimen span of 2200 mm is used. Then, the displacement of specimen span center until destruction and the axial force introduced into the PC steel were measured with a load cell. Loading was performed by load control, and while observing the value of the load indicator attached to the loading device, the rebar yield load was increased in 4 kN steps and then removed in 8 kN steps. After the test was completed, cores were taken from the positions (▨) shown in figure 5 and subjected to a compressive strength test including a static elastic modulus test.

Table 4: Material test results using core collected from each degradation process

Specimen name	Accelerated curing period (days)	Material test result of collected core			
		Compressive strength (N/mm²)		Modulus of static elastic (N/mm²)	
		Upper edge side	Lower edge side	Upper edge side	Lower edge side
No.0	45※	37.6	38.1	28723	28677
No.1	21	38.3	38.5	32450	29012
No.2	105	33.2	37.9	16455	28431
No.3	406	30.7	31.8	11433	17566
No.4	700	29.1	28.9	10932	11098

※The value of PC No.0 indicates the aerial curing period.

3.3.1 Material test results of the sampled core

Table 4 shows the compressive strength and static elastic modulus test results using φ100 × 200 cores collected from a total of 5 specimens from №0 to №4. Although the compressive strength showed a slight decreasing tendency in the order of №0→№4, the tendency was gradual, and almost no difference in compressive strength was observed the upper edge and lower edge cores. On the other hand, the static elastic modulus showed a tendency to increase from №0 to №1 on the upper edge side, and then a large decreasing tendency was confirmed. On the lower edge side, a large decrease tendency can be confirmed from the specimen of №3 in which the static elastic modulus on the upper edge side was slowed down. This shows the same tendency as the monitoring result of the axial reinforcement strain due to the accelerated curing described above, and it can be judged that the restraining effect by the prestressing force of the PC steel was also confirmed on the lower edge side.

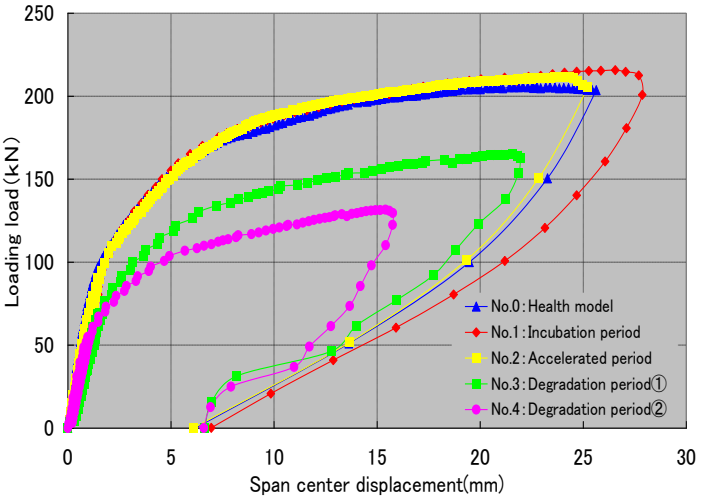

Figure 11: P－δ curve

Table 5: Maximum load and displacement amount

Specimen	Maximum load (kN)	Displacement amount at maximum load (mm)
No.0	203.6	25.6
No.1	200.8	27.9
No.2	205.4	25.2
No.3	162.6	21.9
No.4	129.6	15.8

3.3.2 Loading [destruction] test results

Figure 11 shows the load-displacement curves of a total of five specimens from №0 to №4. Table 5 shows the maximum loading test load and the displacement at the maximum load.

In the sampled core, the static elastic modulus of №0 to №2 was decreased to about 60% of №0 on the upper edge side, but no significant change was observed in the P-δ curve. At the level where the static modulus of elasticity of only the upper edge concrete decreases, the effect on the whole is small, and the effect of tensile force acting on the axial reinforcement and PC steel due to ASR expansion is stronger, so chemical prestress is introduced into the concrete. Thus, it is considered that the load carrying capacity does not decrease even though the static elastic modulus is small. However, in the test specimens (both sides are decreased to about 40% of №0) of №3 and №4 in which the static elastic modulus on the lower edge side was decreased, a significant energy reduction tendency of the P-δ curve was confirmed. It is considered that when the static elastic modulus of the concrete as a whole

decreased uniformly, the prestressing effect of ASR expansion introduced into the concrete caused a significant decrease in load carrying capacity.

3.3.3 Propagation characteristics of Broadband ultrasound

(1)Overview of the Broadband ultrasonic transmission test used

In recent years, regarding the expansion deterioration of concrete caused by ASR, it has been reported that the propagation velocity and frequency characteristics measured by a transmission method using Broadband ultrasonic are effective methods for evaluating the physical properties of concrete[3),4)]. Here, the ultrasonic wave propagation velocity, the energy of the receiving wave, and the frequency characteristics were measured by the transmission method using the Broadband ultrasonic measurement device shown in Figure 12. It has been confirmed that this measuring instrument has a relatively wide frequency component ranging from 0 to 500 kHz[4)].

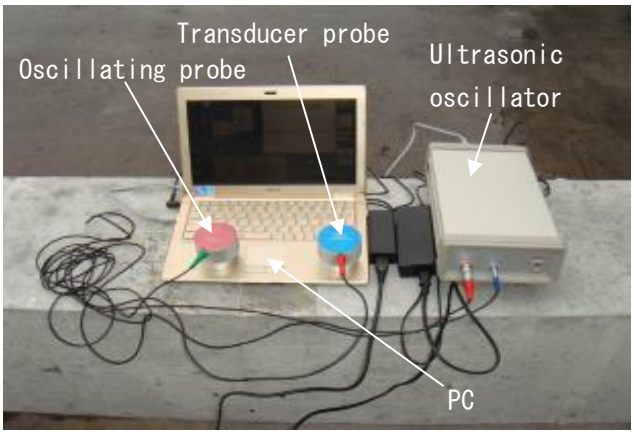

Figure 12: Broadband ultrasonic measurement system

Ultrasonic waves were oscillated and received using two φ40mm Broadband vertical probes incorporating a ceramic vibrator (resonant frequency 0.5MHz) under the measurement conditions of an applied voltage of 30V, an amplification degree of 70dB, and a sampling frequency of 2MHz.

As the evaluation items, the ultrasonic wave propagation velocity obtained from the ultrasonic wave propagation time in the specimen and the frequency distribution obtained by performing the FFT processing on the received waveform were taken up. When the oscillation and receiving probe were installed on the surface of the test piece, the surface was subjected to a grinder treatment to remove the influence of the surface roughness on the test results, and an appropriate contact medium (using Hijet made by SONOTECH) was used. In consideration of the influence of the water content of the specimen on the test results, the specimen was immersed in an aqueous solution until immediately before the test was performed.

(2)ASR material degradation evaluation by ultrasonic propagation behavior

In this study, the effect of the accelerated curing on the propagation behavior of the ultrasonic wave propagating in the specimen during the expansion process of the PC beam specimen was examined. The measurement was performed on a total of four specimens ①before accelerated curing: the specimen on day 0, ②the incubation period: the specimen on day 21, ③the acceleration period: the specimen on day 105, and the ④deterioration period: the specimen on day 700. Figure 13 shows the ultrasonic waveform that propagated through the specimen. The reception amplitude ratio on the vertical axis means a ratio with respect to the maximum amplitude value obtained ①before accelerated curing: day 0. Characteristically, the upper edge side showed a tendency that the maximum amplitude during the incubation period was slightly larger than that before the accelerated curing. Although this was confirmed in the core specimen, it is considered that the expansion pressure resulting from the cubical expansion accompanying the ASR reaction was accumulated inside the aggregate. In addition, it was confirmed that the maximum amplitude tended to decrease significantly from the incubation period to the acceleration period and the deterioration period. On the other hand, on the lower edge side, an increasing tendency of the amplitude width can be confirmed until the acceleration period, and the amplitude is significantly decreased at the stage of the deterioration period. This can be determined to be the effect of the constraining effect due to the prestressing force of the PC steel material arranged on the lower edge side. Figure 14 shows the result of performing the frequency of the obtained received waveform. On the upper edge side, the frequency component around 100kHz tended to increase during the incubation period compared to before the accelerated curing, and a significant decrease tendency of this frequency component was confirmed during the acceleration period and the deterioration period. On the lower edge side, the frequency distribution tended to be similar up to the acceleration period, and a significant decrease tendency of the frequency component was confirmed in the deterioration period.As described above, it was confirmed that the lower edge side had a slow tendency to decrease the frequency band after 100kHz than the upper edge side due to the constraint effect of the prestressing force of the PC steel. The P-δ curve obtained by the destructive test in Figure 11 shows almost the

same hysteresis curve until the acceleration period. Therefore, in the PC girder, as long as the expansion is suppressed by the ASR on the lower edge side, the effect of decrease the load-bearing performance is considered to be very low. The ultrasonic wave propagation velocity of the PC beam specimen is the width: 300mm of the specimen remove by the propagation time of the rising part of the received waveform in Figure 13, and is in the range of 3.319 to 4.167km/sec. Considering this propagation speed, the wavelength of the ultrasonic wave corresponding to 100 to 150kHz with large

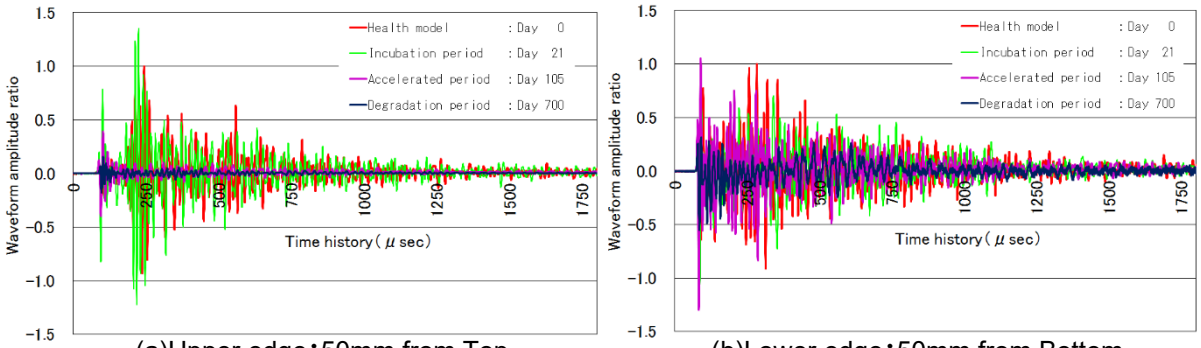

(a)Upper edge；50mm from Top (b)Lower edge；50mm from Bottom

Figure 13: Received waveform measured by transmission method

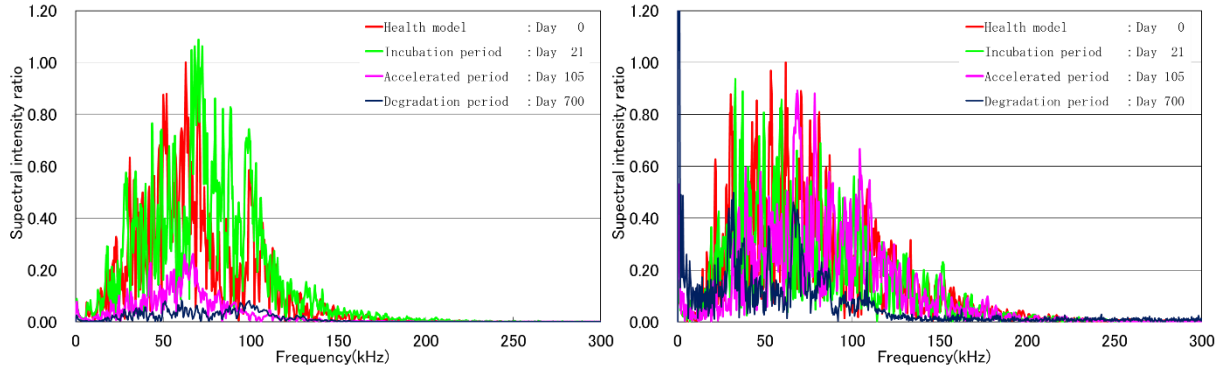

(a)Upper edge；50mm from Top (b)Lower edge；50mm from Bottom

Figure 14: Frequency analysis result of received waveform

attenuation is 22 to 42 mm, which is almost corresponding with the particle size range of the used coarse aggregate: 20 to 35mm. Therefore, it is considered that the frequency attenuation tendency in the range of 100 to 150 kHz during the acceleration period and the deterioration period is due to the presence of aggregate cracks generated in the specimen. Here, as the aggregate crack, there are generally three types of cracks in the concrete structure: an aggregate crack, a mortar crack, and a bond crack. The authors analyzed the crack density by cross-sectional observation during the ASR expansion process using the core specimen and confirmed that in the case of ASR, aggregate cracks were dominant.[5)]

Here, Figure 15 shows the results of the compressive strength and static elasticity tests and the ultrasonic wave propagation behavior which were carried out earlier, arranged from the viewpoint of the

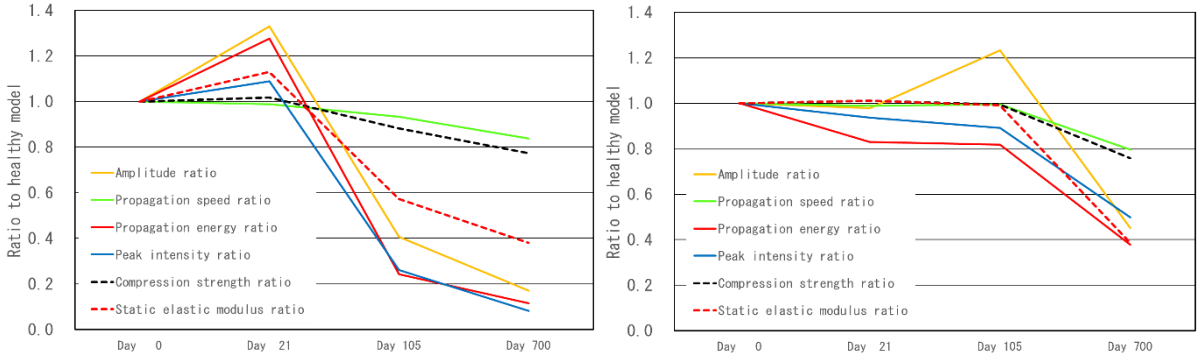

(a)Upper edge；50mm from Top (b)Lower edge；50mm from Bottom

Figure 15: Relationship oy each evalution index to deterioration grade

ASR deterioration grade of the PC beam specimen. The maximum amplitude used for the evaluation index indicates the absolute value of the maximum and minimum values of the received waveform. The received wave propagation energy indicates the frequency distribution in the frequency range of 0 to 300kHz and the area of the portion surrounded by the transverse axis, and the peak intensity indicates the frequency value with respect to the maximum spectrum intensity. The transverse axis in the figure indicates the deterioration grade due to accelerated curing, and the longitudinal axis indicates the ratio of the value obtained in each deterioration grade process to the value before accelerated curing in order to make the comparison the same level. Generally, the relationship between the ultrasonic wave propagation velocity, the static elastic modulus and the compressive strength is represented relational expression by the following equations (1) and (2). We confirmed the result, Although the correlation between the two was considered to be high, the ultrasonic wave propagation velocity was highly correlated with the compressive strength from this Figure 15, and the propagation behavior [maximum amplitude, propagation energy, peak intensity] obtained from the frequency analysis was highly correlated with the static elastic modulus. This indicates that the static elastic modulus is more sensitive than the compressive strength to the presence of cracks in the test specimen generated by accelerated expansion. From these results, it was determined that it was difficult to evaluate the ultrasonic wave propagation velocity in the case where cracks occurred in the concrete due to ASR, and it was extremely important to evaluate the frequency characteristics obtained from the propagation waveform.

$$E_c = 1.04 \cdot \frac{(1-2\nu_c)(1+\nu_c)}{1-\nu_c} \cdot \rho_c \cdot V_c^2 - 12.0 \quad (1)$$

$$\sigma_c = 60 \cdot \left(\frac{E_c \cdot (2.4)^2}{k \cdot 33.5 \cdot \rho_c^2} \right)^3 \quad (2)$$

Ec: Static modulus of elasticity(kN/mm^2)

ν c : Poisson's ratio ν c=0.20

ρ c : Density ρ c=2.4(g/cm^3)

σc: Estimated compressive strength(N/mm^2)

Vc : Ultrasonic wave propagation speed(km/sec)

k : Correction factor for material used k=1.00

4. Confirmation of deterioration behavior of railway PC girder due to ASR progress

4.1 Overview of PC track girder

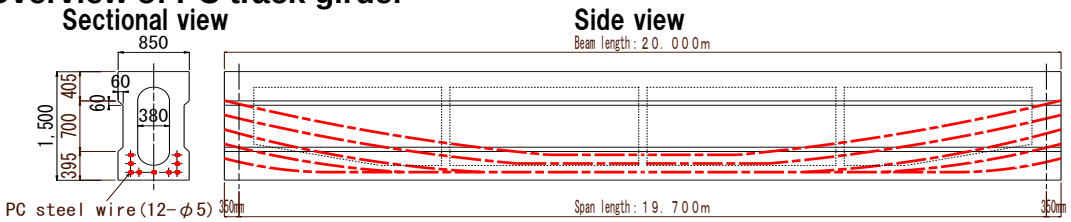

Figure 16: PC track girder

The PC track girder is a simple girder (Figure 16) with a span length of 19.300m by the Freyssinet system. The design standard strength of concrete is σck=45N/mm^2, nine PC steel wires 12φ5 are arranged (end section anchorage), and a prestress force of σp=750N/mm^2 is introduced as the PC steel wire stress degree.

4.2 PC track girder upper and lower edge strain monitoring measurement and other results

The girder was completed in 1985 and a detailed survey in 2002 confirmed the ASR. Based on this, since 2003, strain fluctuations (Figure 17) at the upper and lower edges of PC track girder have been monitored. For the strain measurement, an optical fiber sensor with a length of 2.000m using the principle of microbending[5] was installed at the center of the span, and the change ratio to the length was measured as strain. Although the strain generated before the measurement was unknown, the release strain measured by cutting the internal axial reinforcement using the stress release method was set as the

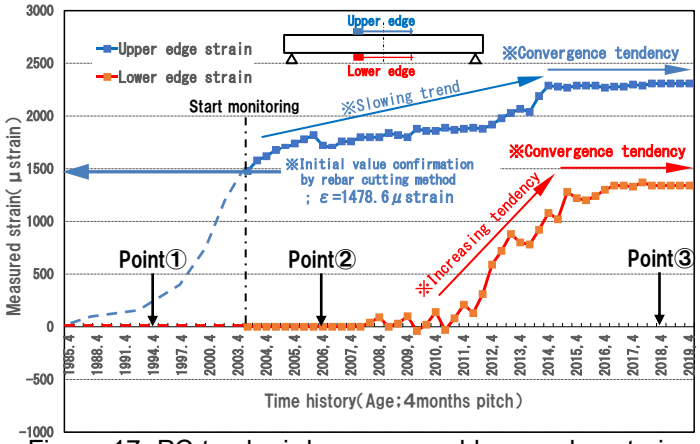

Figure 17: PC track girder upper and lower edge strain fluctuation by monitoring

current strain. As in the case of the PC beam test, it was confirmed that the strain on the lower edge side tends to increase when the strain fluctuation on the upper edge side slows down. Figure 19 shows the results of measuring the propagation waveform (Figure 18) and performing frequency analysis in the transmission method test using Broadband ultrasound conducted at points ① to ③ in Figure 17.

Point ①(1994) can be estimated to be the stage of transition from the incubation period to the acceleration p eriod, and there was no confirmed significant difference in the total energy of the received waves on the upper and lower edges. In the acceleration period of Point ②(2006), the total energy on the upper edge side was significantly decreased, but the lower edge side was at the same level as Point ①. It can be confirmed that in the deterioration period of point ③(2018), the total energy on the lower edge side has also been significantly decreased. The level converged to almost “zero” in all frequency bands, and it was determined that the progress of ASR had converged.

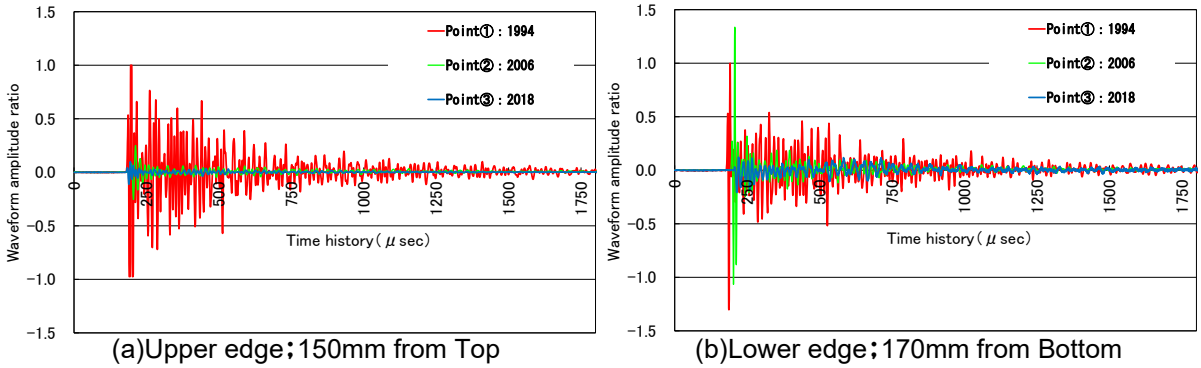

(a)Upper edge；150mm from Top (b)Lower edge；170mm from Bottom

Figure 18: Received waveform measured by transmission method

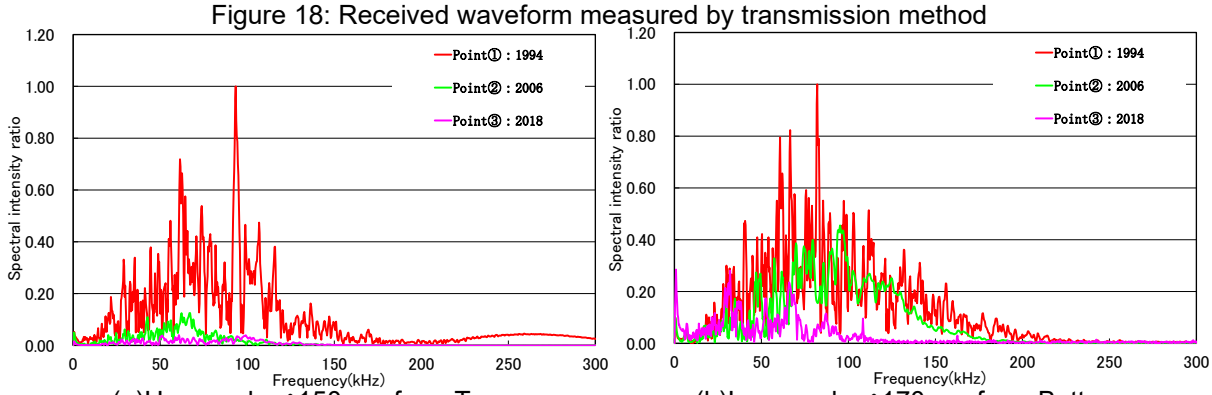

(a)Upper edge；150mm from Top (b)Lower edge；170mm from Bottom

Figure 19: Frequency analysis result of received waveform

4.3 Evaluation of load bearing performance of PC girder under constant load

An increase in the strain at the lower edge means that the PC steel wire bears additional tensile stress. Also, judging from the frequency characteristics obtained from the analysis of the propagation waveform of the Broadband ultrasonic wave, there was a concern that the static elastic modulus of concrete would be significantly decreased. Although it is difficult to carry out a destructive test as in the case of a PC beam specimen, a loading test(Figure 20) using a quantitative load was carried out because the progress of ASR is sensitive to the static elastic modulus. Then, the load bearing performance was evaluated by measuring the displacement of the center of the span of the main girder. Figure 21 shows, the results of displacement measurement and the results of the compressive strength and static elastic modulus tests by core sampling performed at points ① to ③ shown in Figure 17. The initial expectation was that if the static elastic modulus decreases over time, the generated displacement will necessarily increase. However, the obtained results indicate that the static elastic modulus: Ec obtained by core sampling is significantly decreased with the passage of time, but the fluctuation of the static displacement: δ tends to be very small (refer to the red dotted line in

Figure 20: Loading test 14.5tf vehicle

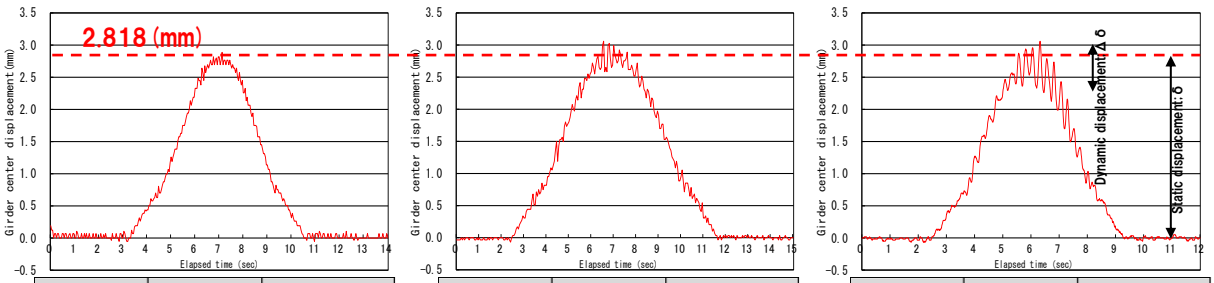

Δ δ	δ	Impact effects Δ δ / δ
0. 193 (mm)	2. 818 (mm)	0. 068

σck (N/mm²)		Ec (N/mm²)	
Upper edge	Lower edge	Upper edge	Lower edge
44. 3	45. 7	32780	33282

(a)Point①：1994

Δ δ	δ	Impact effects Δ δ / δ
0. 476 (mm)	3. 060 (mm)	0. 156

σck (N/mm²)		Ec (N/mm²)	
Upper edge	Lower edge	Upper edge	Lower edge
41. 1	43. 9	21622	31176

(b)Point②：2006

Δ δ	δ	Impact effects Δ δ / δ
0. 799 (mm)	3. 060 (mm)	0. 261

σck (N/mm²)		Ec (N/mm²)	
Upper edge	Lower edge	Upper edge	Lower edge
34. 2	34. 8	9621	10210

(c)Piont③：2018

Figure 21: Dsplacement of girder center span by dynamic loading test and static elastic modulus test result using core

Figure 21:2.818mm). From these results, it was judged that it was difficult to evaluate the load-bearing performance based on the change in the displacement. The authors paid attention to the fact that the dynamic displacement: Δδ significantly changed in three measurements. The impact effect obtained by remove the dynamic displacement: Δδ by the static displacement: δ was confirmed to be , point ①: 0.068→point ②: 0.156→ point ③: 0.261, indicating a large increasing tendency. As shown in Figure 22, it was confirmed that this impact had periodicity, and it was considered that the natural frequency of the PC track girder could be confirmed by analyzing the frequency of this component.

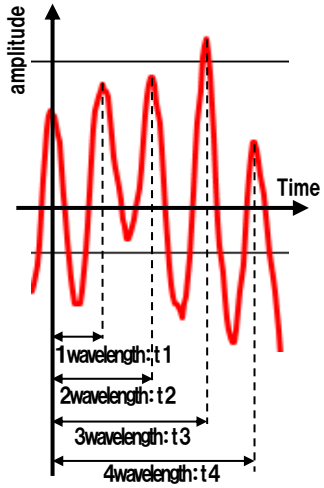

Figure 22: Periodicity of impact effects

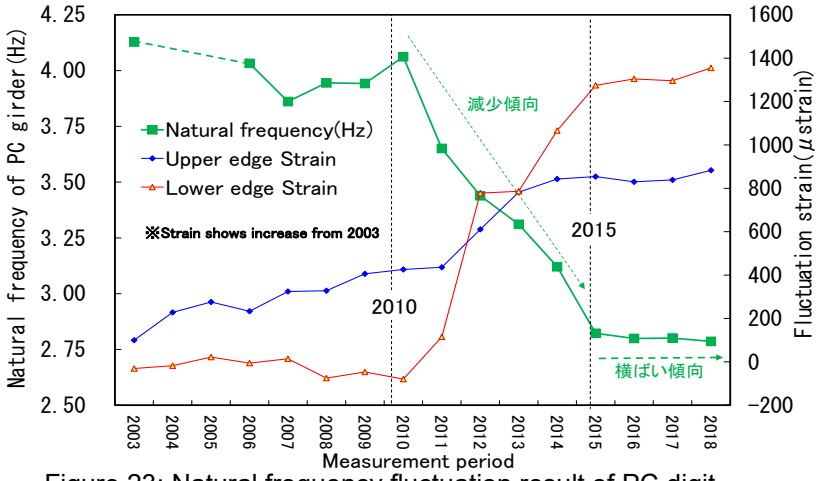

Figure 23: Natural frequency fluctuation result of PC digit obtained from displacement measurement waveform

The loading test has been performed every year since 2003, and Figure 23 shows the relationship between the natural frequency obtained by frequency analysis of the obtained displacement waveform and the increase of the upper and lower edge strain since 2003. The natural frequency of the PC track girder calculated from the standard cross section and the design conditions at the time of design was “4.874Hz”. Until 2010 when the lower edge strain increased, the natural frequency obtained from the loading test tended to be slightly lower. From 2010, it can be confirmed that the natural frequency obtained from the

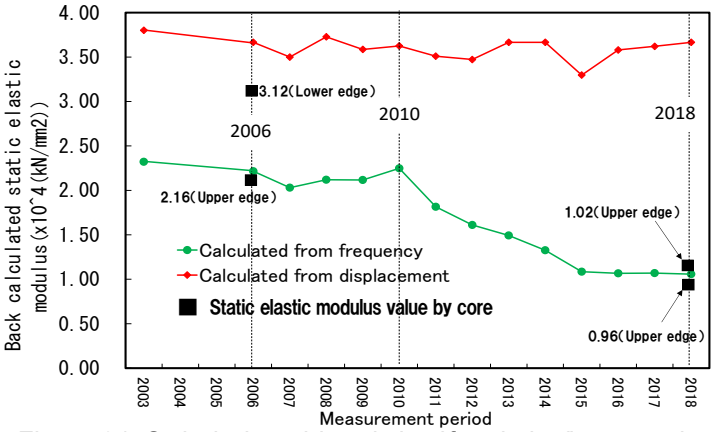

Figure 24: Static elastic modulus calculated from the loading test results

loading test has started to decrease as the lower edge strain increases. Figure 24 shows the result obtained by back calculating the static elastic modulus from the displacement and natural frequency obtained by the loading test. As described above, there is almost no change in the static elastic modulus obtained from the displacement, but the static elastic modulus obtained from the natural frequency shows a decreasing trend since 2010. In addition, when the static elastic modulus values obtained by core collection in 2006 and 2018 shown in Figure 21 were plotted, it was confirmed that the values approximated to a static elastic modulus(■ in Figure 24) curve calculated backward from the frequency. From the above, it was determined that if the natural frequency of the PC track girder could be managed, the static elasticity coefficient which had a large effect on the main girder rigidity could be evaluated. That is, it was determined that the load-bearing performance could be grasped.

Laser irradiation distance	～70 (m)
Sampling frequency	～500 (Hz)
Power supply	AC100V
Operating temperature limit	-10～55℃

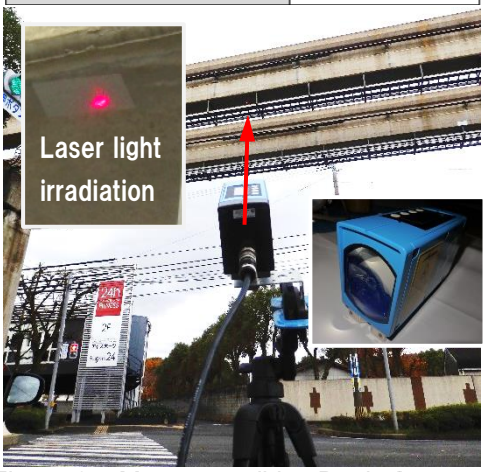

Figure 25: Measurement with laser Doppler vibrometer

5. Proposal of load-bearing performance evaluation method with ASR progress of PC track girder

From the test specimens conducted so far and the verification with actual structures, it is considered important to accurately evaluate the fluctuation of the static elastic modulus in order to evaluate the load-bearing performance accompanying the progress of ASR. Factors sensitively responding to the fluctuation of the static elastic modulus include the fluctuation of ①the upper and lower edge distortion and the ②natural frequency. However, monitoring of the fluctuation of ②the upper and lower edge distortion requires constant monitoring. There are hundreds of PC track girder on the route, and it is extremely expensive and practically difficult to perform strain monitoring of all main girder. Therefore, the main focus was on measuring the natural frequency of the PC track girder to evaluate the static elastic modulus. As the evaluation method, the natural frequency of the PC track girder was measured using a laser doppler vibrometer shown in Figure 25.This vibrometer uses a visible red laser and is a system that can measure the vibration [displacement] of a structure in real time without contact. By using a high-precision frequency band with a sampling frequency of 500 Hz, it is possible to accurately measure a dynamic response such as a natural frequency of a structure. It is easy to carry, can measure all target digits with one unit, and can evaluate quickly at low cost.

At present, the natural frequency fluctuations of 11 PC orbital girder designated as important management girder are managed using this measurement system.

Acknowledgments

In summarizing this paper, we received valuable advice from Kitakyushu High-speed Railway Co., Ltd. and other related parties. We show them respect.

Bibliography;

1) Shigeru Matsumoto;Report on long-term follow-up inspection results of surface protection work for alkali-aggregate reaction, Dissertation report collection of the Symposium on repair, reinforcement and upgrade of concrete structures, Volume 2, pp.29-34、2002

2)Midori Onozato;Physical property test and component test of reinforced concrete members with alkali-aggregate reaction, Annual papers of concrete engineering, Vol.29, №1, pp.1311-1316, 2007

3)Yusuke Nakagawa;Study on prediction method of concrete physical property by ultrasonic method, Annual papers of concrete engineering, Vol.28, No1, pp.1889-1894, 2006

4)Munenobu Murasaka;Application of ultrasonic method to evaluation of material deterioration of concrete with ASR, Annual papers of concrete engineering, Vol.35, No1, pp.1735-1740, 2013

5)Munenobu Murasaka;Report on behavior characteristics of PC beam specimen during loading test using optical sensor, Papers of Japan Society of Civil Engineers, Vol.63, pp.1031-1032, 2008